Programming Projects in Molecular Modeling

Project 5

Mahdi Torabi, Md. Shafayet Islam, Iris Tamsalu

April 29, 2025

Contents

1 Introduction

This project reflects our effort to reproduce data acquired through experimental techniques via the simulation techniques we have learned. Since the molecular dynamics (MD) simulation we use has only the Lennard-Jones potential (LJ), the choices were limited. Our system had to be neutral, with no interatomic interactions besides van der Waals interactions. The decision was made to simulate a noble gas, Argon to be particular, and study its phase diagram and compare it to the experiment. We also attempted to measure the viscosity of Argon, which will be discussed in section 3.

The code is provided in the supplementary material, available at the following GitHub repository: `github.com/iristamsalu/KEM381_project5`. All usage instructions are provided in the `README` file.

2 Argon Gas-Liquid Coexistence Curve

LJ parameters for Argon were taken from the work of Song-Hi Lee [1]:

- $\sigma = 0.34\,\mathrm{nm}$ — the characteristic distance where the interatomic potential crosses zero, effectively representing the size of an Argon atom.

- $\varepsilon/k_\mathrm{B} = 120\,\mathrm{K}$ — the depth of the potential well, corresponding to the strength of the van der Waals interactions between Argon atoms, expressed in temperature units.

- $r_\mathrm{c} = 0.85\,\mathrm{nm}$ — the maximum distance beyond which the interatomic interactions are neglected in the simulation.

Once the LJ parameters were set in `config.py`, all the simulation parameters were set to real units. A series of MD simulations with the NVT ensemble were conducted to explore the phase behavior of Argon and compare it to the experiments conducted by Michels et al. [2], and their reported phase diagram can be seen in fig. 1. The same experimental data can also be found in fig. 2, where the units are perhaps more intuitive. The paper reported the following critical temperature and density:

- Critical temperature: $T_\mathrm{c} = -122.29°\mathrm{C} = 150.86\,\mathrm{K}$

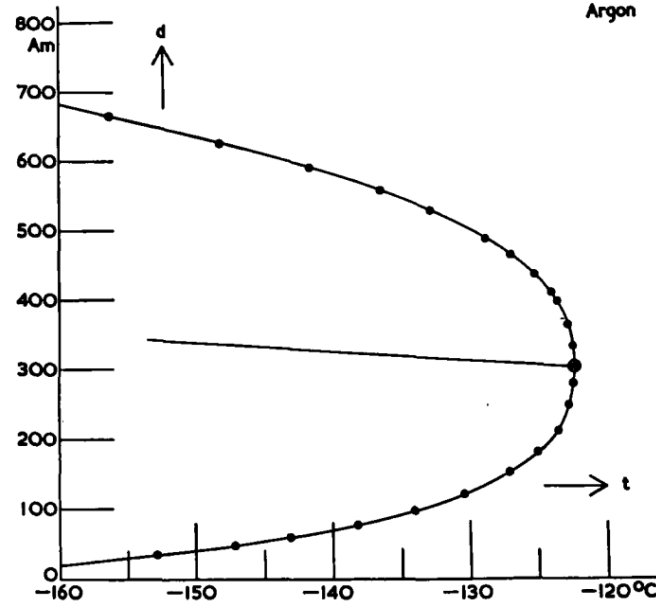- Critical density: $\rho_\mathrm{c} = 300.4\,\mathrm{amagat} = 535.78\,\mathrm{kg/m^3}$

Figure 1: Phase diagram with the gas-liquid coexistence curve, where the y-axis is the density in amagat unit (1 Am = 1.783558 $\frac{kg}{m^3}$) and the x-axis is the temperature in °C.
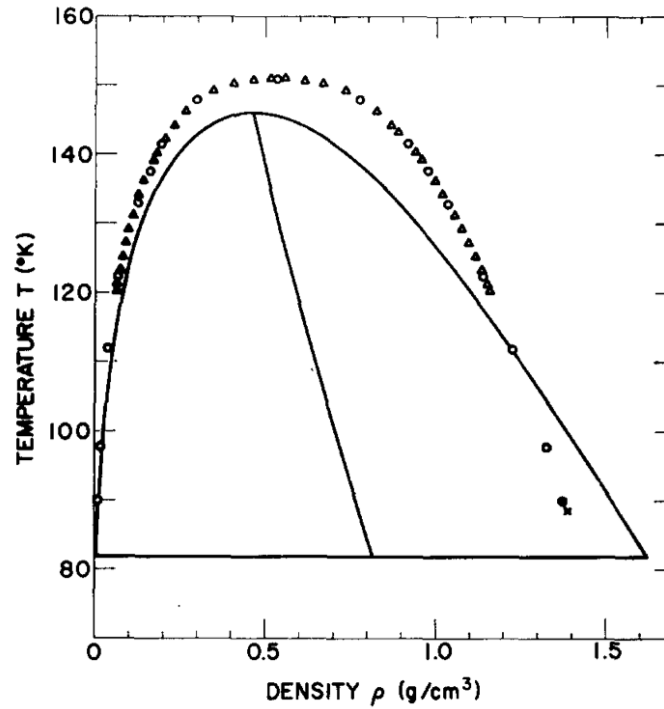

Figure 2: The gas-liquid coexistence curve. The y-axis is density in $\frac{g}{cm^3}$ and the x-axis is temperature in Kelvin. The solid curve is modeled by Henderson and Wertheim [3]. Experimental data is marked with different symbols. The experimental data by Michels et al. [2] is marked with triangles.

All the simulations had a step size of 1 femtosecond (fs) and were run for 50,000 steps. The Langevin thermostat was used with a thermostat constant equal to $0.5 \times 10^{-12} \frac{kg}{s}$. All the temperatures are in Kelvin and all the densities are in $\frac{kg}{m^3}$.

To evaluate the validity of our parameters and the simulation program code, three points from the phase diagram were taken as follows:

1. Gas phase: T = 148.15 K, Density = 89.1779 kg/m³

2. Coexistence-phase, liquid-like: T = 123.15 K, Density = 891.779 kg/m³

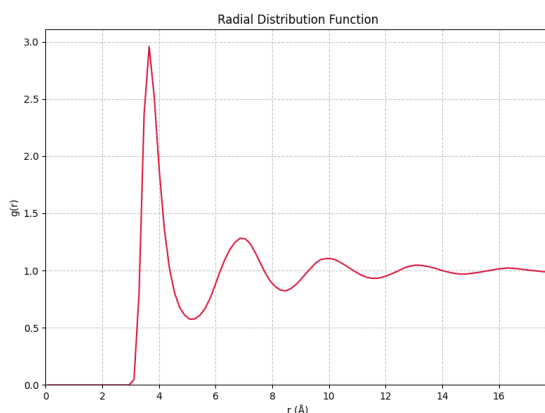3. Liquid phase: T = 110.0 K, Density = 1500.0 kg/m³

The results are in figs. 3a to 3c. The results agree with the experimental data and show the phase behavior correctly. The phase behavior was studied with the radial distribution function (RDF). The program for RDF is in `rdf.py` and the videos are in `/videos`.
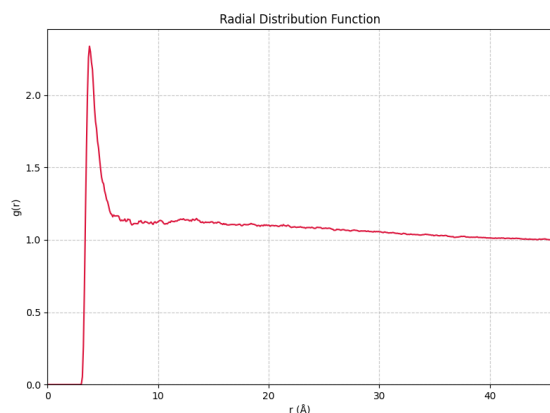
(a) Gas phase: density $= 89.18\,\text{kg/m}^3$, $T = 148.15\,\text{K}$.
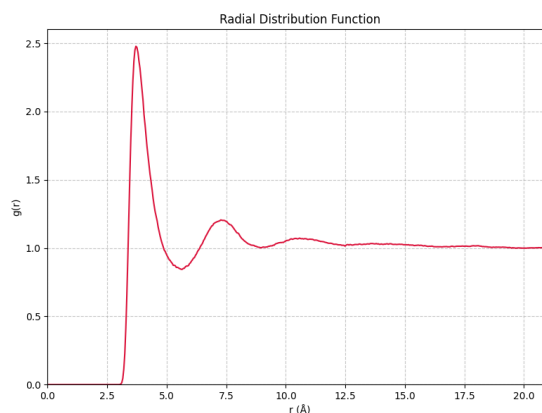
(b) Coexistence, liquid-like: density $= 891.78\,\text{kg/m}^3$, $T = 123.15\,\text{K}$.

(c) Liquid phase: density $= 1500.0\,\text{kg/m}^3$, $T = 110.0\,\text{K}$.

Figure 3: Radial distribution functions (RDFs) from MD simulations (NVT ensemble) of Argon in gas, liquid-like coexistence and denser liquid phases.

Next, a simulation run using the reported critical temperature and density was carried out, and the results are in fig. 4. RDF should show a structure characteristic of the critical region, which is an intermediate structure reflecting large fluctuations. The video of Ar particles at critical point is in `/videos`.
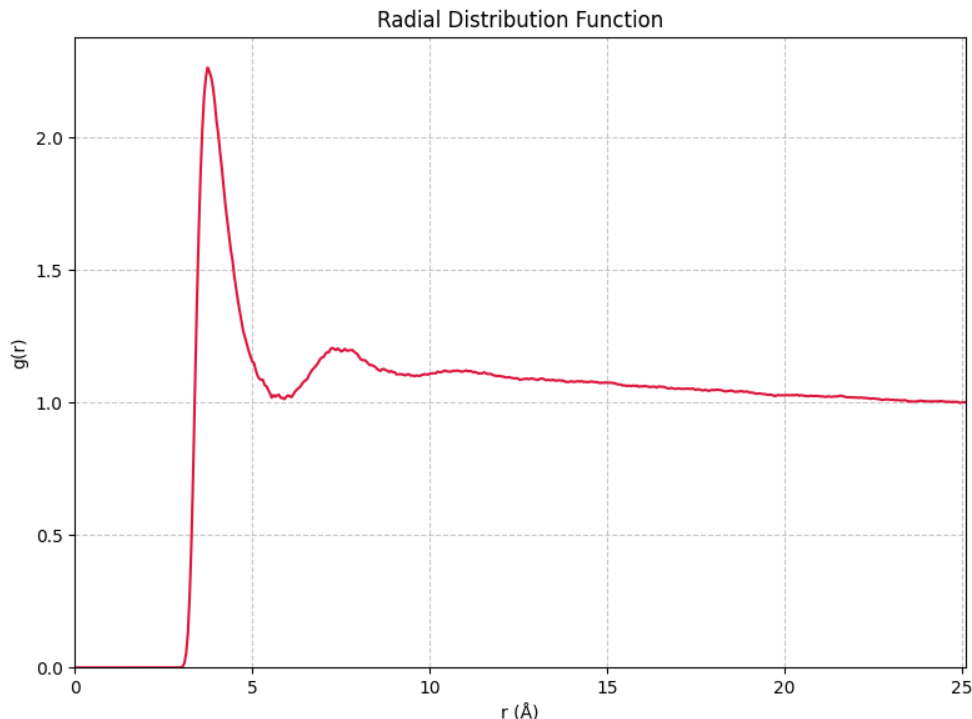

Figure 4: RDF for MD simulation (NVT ensemble) of Argon using the reported critical values: density = 535.78 kg/m^3, T = 150.86 K.

The critical density line in fig. 1 was also followed and investigated, and the results are in fig. 5. We can see in the figure that once the temperature reached 160.86, the RDF started to shift toward the gas phase.

The critical temperature density neighborhood was also investigated by taking higher and lower densities and investigating their RDF plots. The results are in fig. 6.
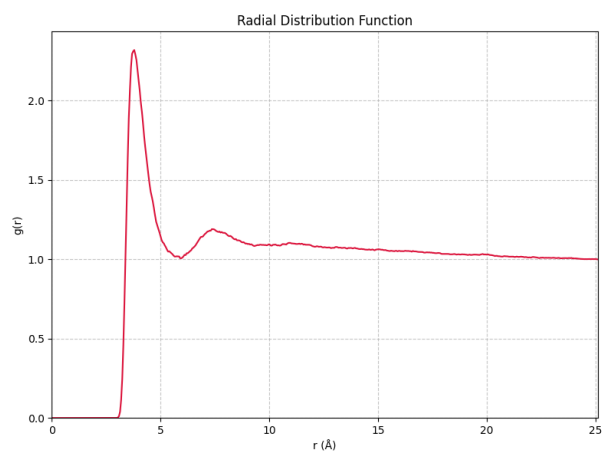
In addition, one final MD simulation was performed in the region of very high density (1248.49 $\frac{kg}{m^3}$) and relatively high temperature (153.15 K), and we observed liquid-like RDF. In this area, Argon is a supercritical fluid (fig. 7).
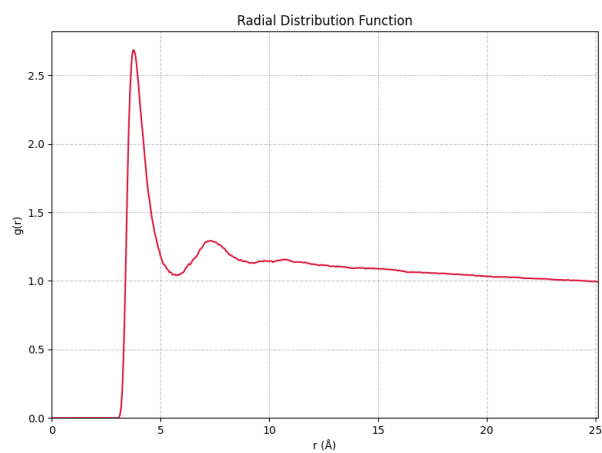
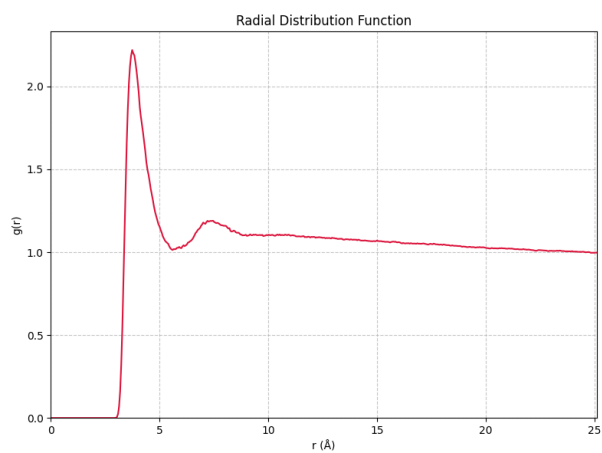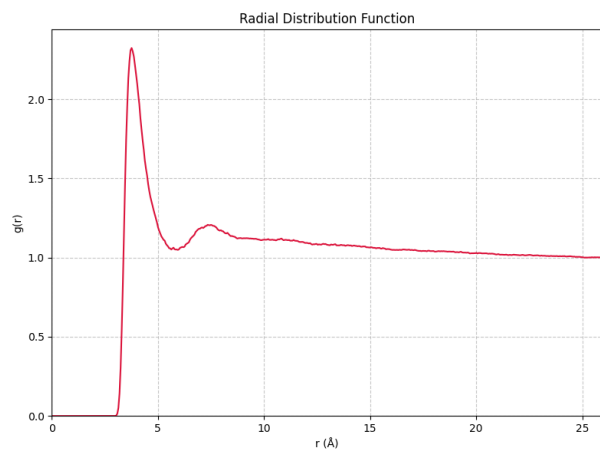(a) T = 120.15 *K*
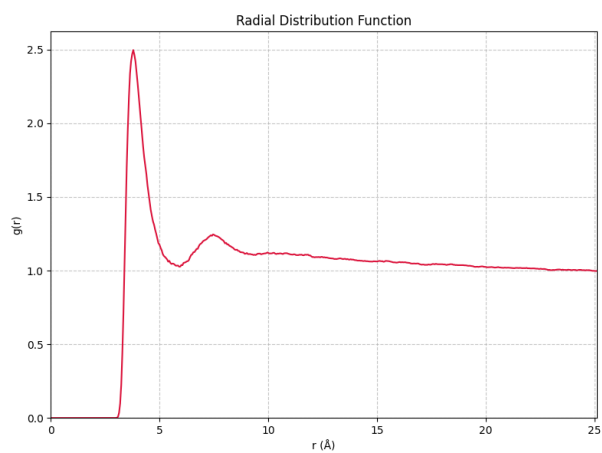
(b) T = 130.15 *K*

(c) T = 140.15 *K*

(d) T = 160.15 *K*

Figure 5: The RDF plots of Argon phase using critical density and different temperatures.

(a) D = 485.7808 kg/m^3
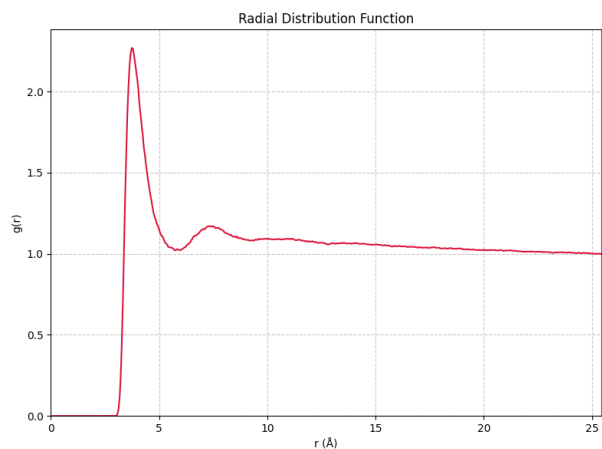
(b) D = 515.7808 kg/m^3
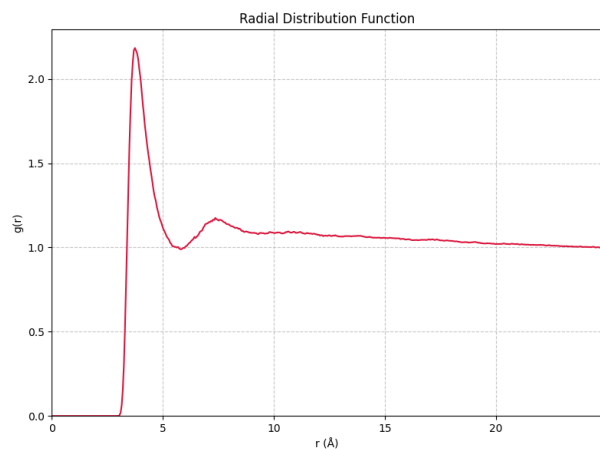
(c) D = 555.7808 kg/m^3
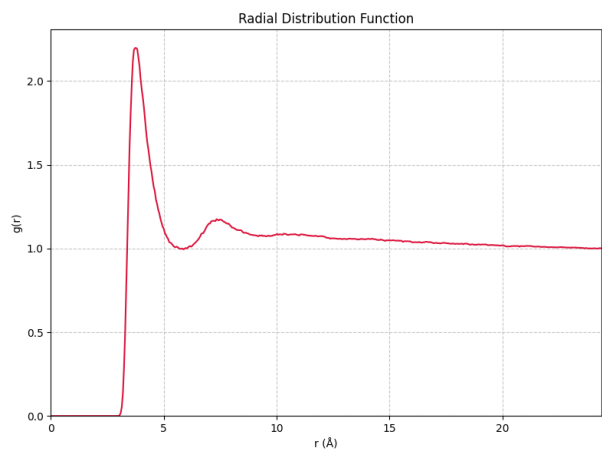
(d) D = 585.7808 kg/m^3

Figure 6: The RDF plots of Argon phase using critical temperature and different densities.

Figure 7: RDF from MD simulation of Argon with density $= 1248.49 \frac{kg}{m^3}$ and temperature $= 153.15$ K. The RDF reflects dense supercritical fluid.

3 Attempts to Measure Viscosity

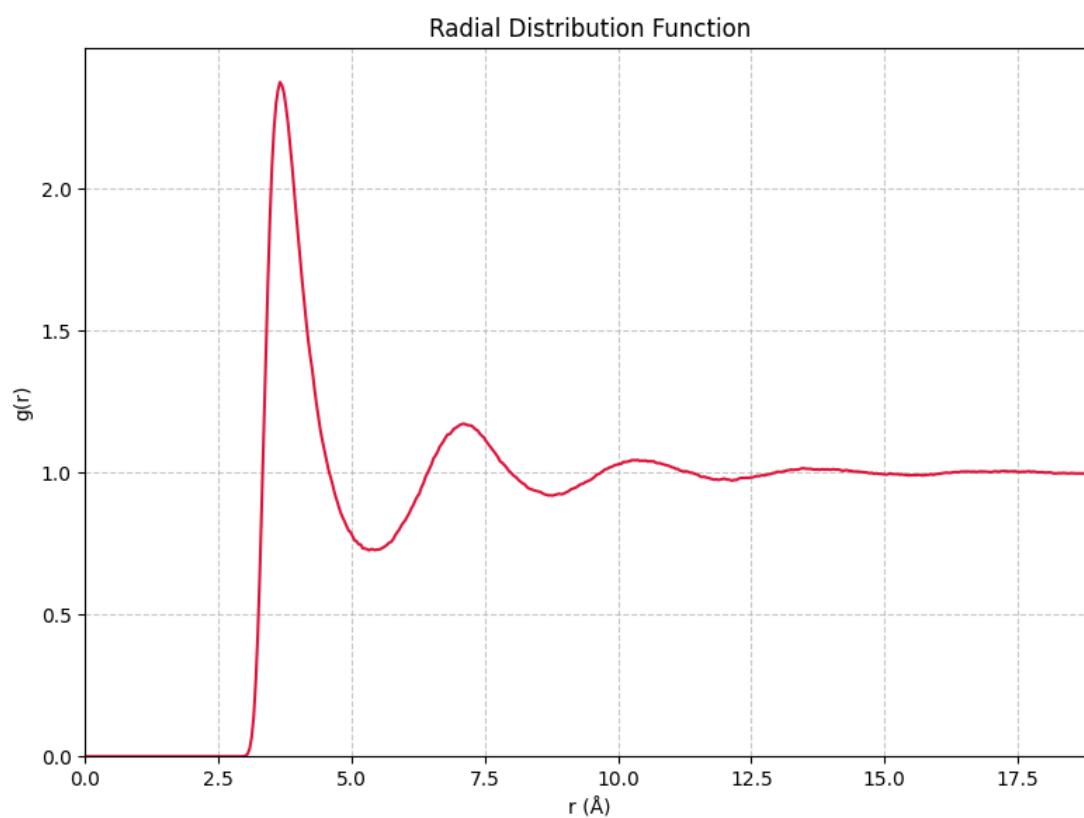In addition to investigating the Argon phase diagram, we made a few attempts to reproduce the experimental viscosity values at different temperature and density combinations from a paper by Haynes 1973 [4]. In this paper, the coefficient of shear viscosity of fluid Argon was measured with a torsional crystal viscometer at temperatures 85-298 K and pressures up to $34 \frac{MN}{m^2}$. The accuracy of these measurements was estimated to be 2%, and the precision was 0.5%.

3.1 Measuring viscosity with Green-Kubo method

We used the Green-Kubo method to calculate viscosity [5]–[7]. To implement this, we modified our MD model's `compute_forces_virial()` function in `forces.py` module and implemented a new function `update_pressure_tensor()` to `simulation.py` module. Instantaneous stress tensor components ($P_{\alpha\beta}$) are calculated at each step using both kinetic energy and the virial sum.

$$P_{\alpha\beta}(t) = \frac{1}{V} \left(\sum_{i=1}^{N} m_i v_{i,\alpha}(t) v_{i,\beta}(t) + W_{\alpha\beta}(t) \right)$$

where $W_{\alpha\beta}(t) = \sum_{i=1}^{N} \sum_{j>i} r_{ij,\alpha}(t) F_{ij,\beta}(t)$ is the virial sum component calculated by the `compute_forces_virial()` function.

Stress fluctuation ($P'_{\alpha\beta}$) is the deviation of the stress from its average value.

$$P'_{\alpha\beta}(t) = P_{\alpha\beta}(t) - \langle P_{\alpha\beta} \rangle$$

For off-diagonal terms $\alpha \neq \beta$, the average $\langle P_{\alpha\beta} \rangle$ should ideally be zero.

Stress autocorrelation function (SACF, $C_{\alpha\beta}(t)$) measures how correlated the stress fluctuations are with themselves over time t.

$$C_{\alpha\beta}(t) = \langle P'_{\alpha\beta}(0) P'_{\alpha\beta}(t) \rangle$$

The Green-Kubo formula for shear viscosity (η) relates viscosity to the time integral of the average off-diagonal SACF ($C_{avg}(t)$).

$$\eta = \frac{V}{k_B T} \int_0^\infty C_{avg}(t) dt$$

where $C_{avg}(t) = \frac{1}{3} \left(C_{xy}(t) + C_{xz}(t) + C_{yz}(t) \right)$ is the average SACF. The script approximates the integral $\int_0^\infty \ldots dt$ by integrating up to a finite time t_{max} where the integral probably converges. SACF and shear viscosity calculations are implemented in `green_kubo.py`.

3.2 Measuring Viscosity with NVT

The first attempts were made with the NVT model. The plateau values were fluctuating significantly, and even more importantly, the plateau, which is essential for viscosity determination using Green-Kubo, collapsed at one point, giving us negative viscosity values. Please find some of the NVT results in fig. 8 and fig. 9. These runs were done at 107.7 K and density=1296.2 kg/m^3, where the experimental viscosity is 1681 $\mu g/(cm \cdot s)$ or 168.1 $\mu Pa \cdot s$. As can be seen from the figures, the viscosity values read from the not-so-stable plateaus varied between $(147.24 - 175.70)\mu Pa \cdot s$. Interestingly, this range does bracket the experimental value, even with unstable plateaus. During all the viscosity runs with NVT, we used the Langevin thermostat with parameter 1.3e-13 $\frac{kg}{s}$.
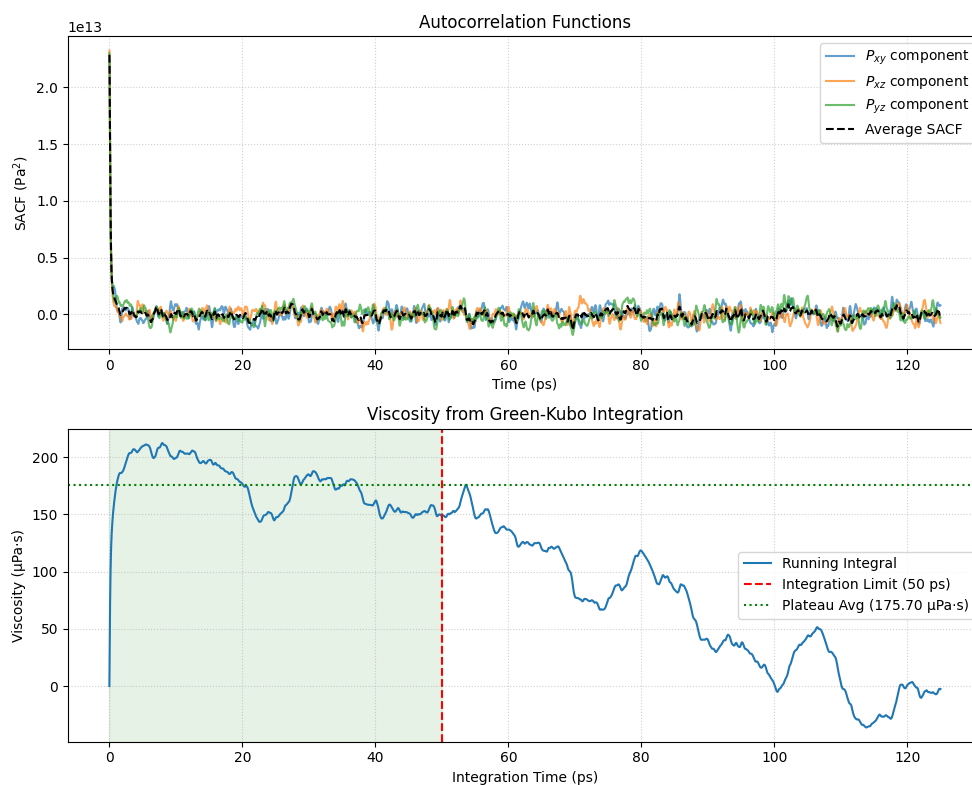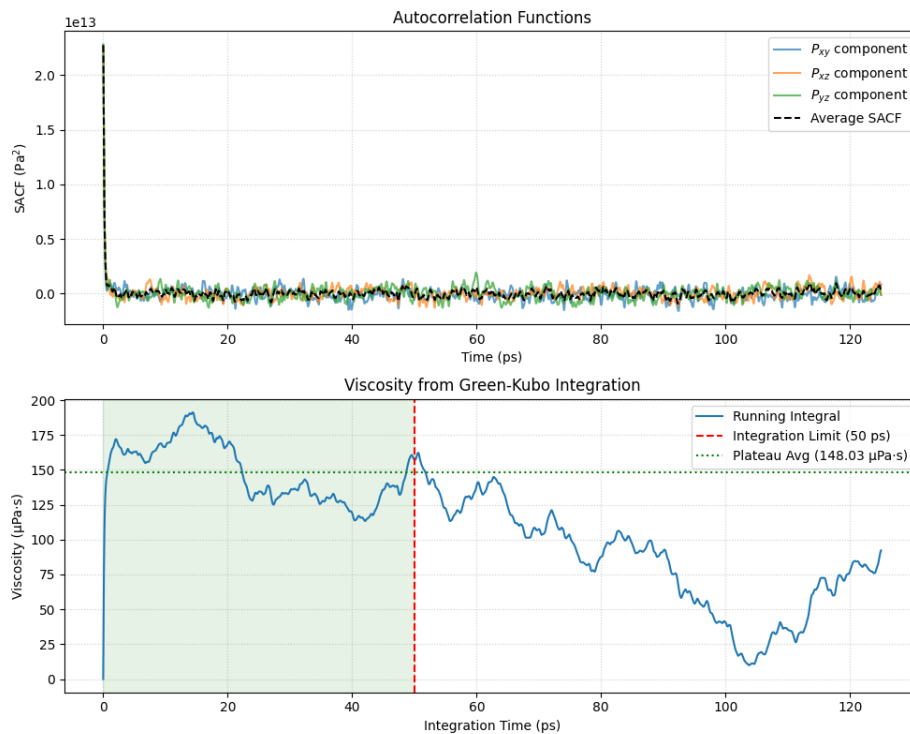

(a) Run I

Figure 8: Part 1 of Green-Kubo viscosity results from NVT model at T=107.7 K and density=1296.2 kg/m^3. Experimental viscosity is 168.1 $\mu Pa \cdot s$.
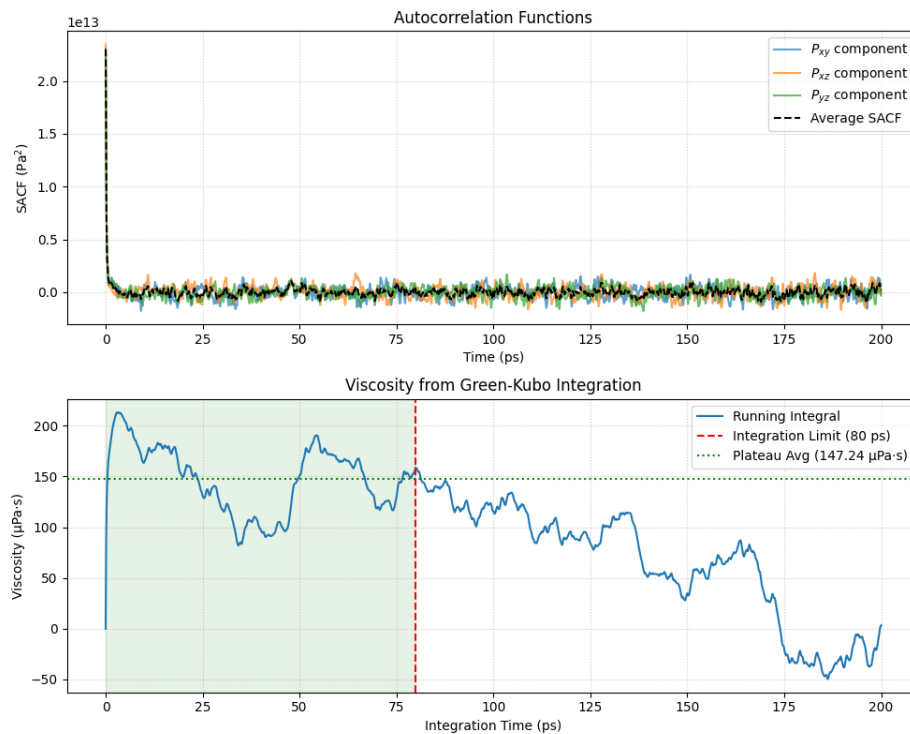
(a) Run II

(b) Run III

Figure 9: Part 2 of Green-Kubo viscosity results from NVT model at T=107.7 K and density=1296.2 kg/m^3. Experimental viscosity is 168.1 $\mu\text{Pa} \cdot \text{s}$.

We also tried to increase the number of particles to get the plateau stable. We did runs with 2000, 3000, and 6000 particles, but did not observe significant improvement. Actually, for 6000 particles, we got significantly higher viscosity values compared to any previous run (almost 300 μPa $\cdot$ s). Possibly due to insufficient equilibration time for the larger system. The results are in fig. 10 and fig. 11.
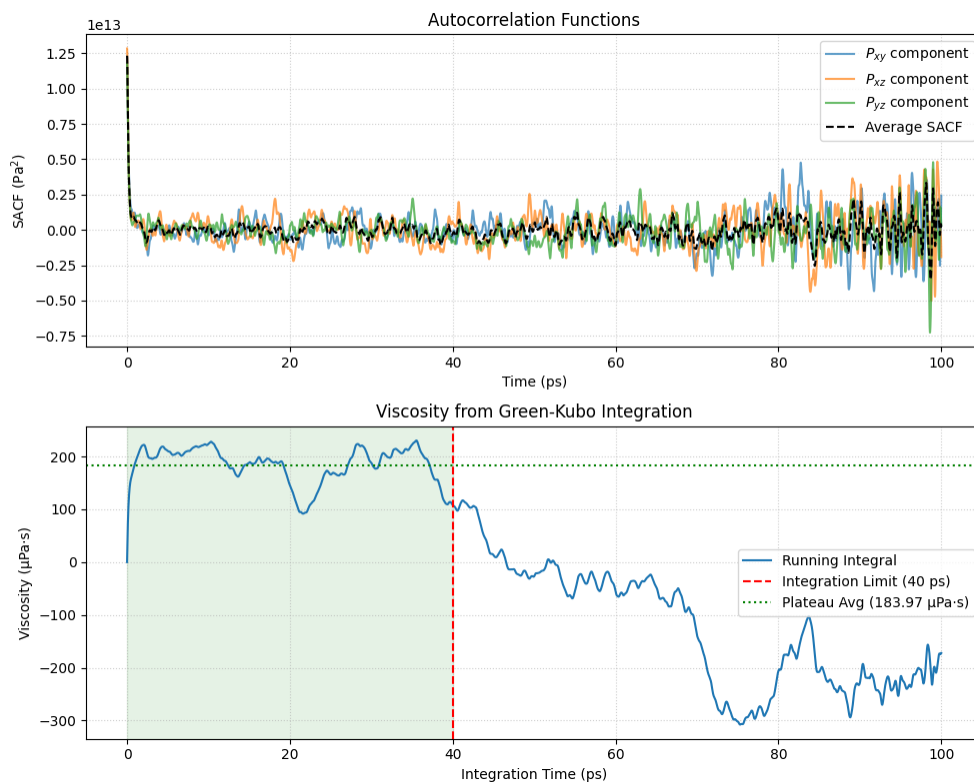
(a) 2000 particles

Figure 10: Part 1 of Green-Kubo viscosity results from NVT model at T=107.7 K and density=1296.2 kg/m^3 with 6000 particles.
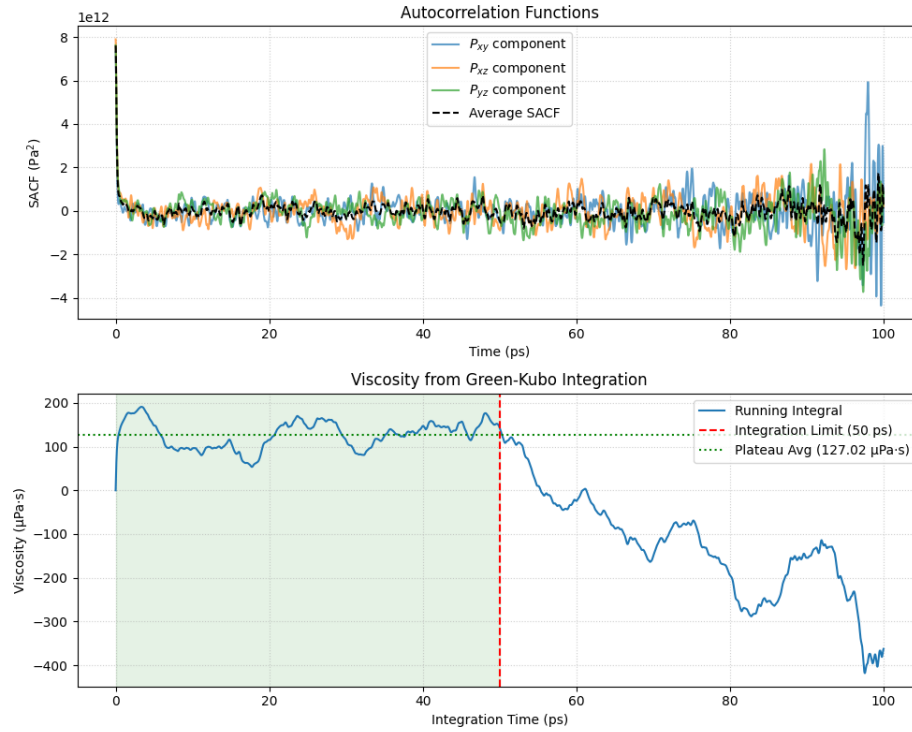
(a) 3000 particles

(b) 6000 particles
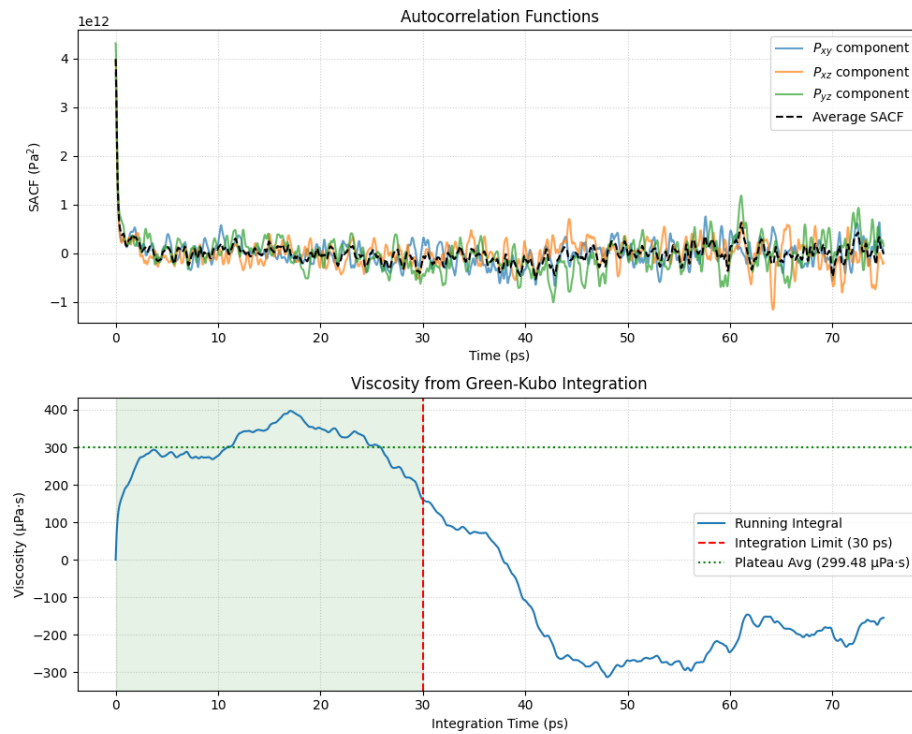
Figure 11: Part 2 of Green-Kubo viscosity results from NVT model at T=107.7 K and density=1296.2 kg/m^3 with 3000 and 6000 particles.

3.3   Measuring Viscosity with NPT-NVT and NPT-NVT-NVE

To achieve a more stable plateau, we introduced a barostat into our simulation. The approach was to set the experimental pressure as the target pressure, then run an NPT simulation until both the pressure and the box volume reached equilibrium. Once equilibrium was achieved, we used the average box volume and particle configuration as the initial conditions for the subsequent NVT simulation. The NPT model uses Nosé-Hoover thermostat and Parrinello-Rahman Barostat, both implemented to thermostats.py. Changes were also made to simulation.py, where we have a new npt_step() function and pressure tracking compute_pressure().

Nosé-Hoover thermostat

The goal of the Nosé-Hoover thermostat is to maintain a target temperature T_{target} by introducing a thermostat variable ζ (friction coefficient) which evolves based on the difference between the current kinetic energy and the target kinetic energy [8].

The equation of motion for the thermostat variable (ζ) describes how the friction coefficient changes based on the temperature deviation. Q is the thermostat coupling constant (or "mass") controlling the response speed.

$$\dot{\zeta}(t) = \frac{1}{Q}\left(\sum_{i=1}^{N} \frac{1}{2}m_i \mathbf{v}_i(t)^2 - \frac{3N}{2}k_B T_{target}\right)$$

Update rule for ζ (Euler integration) is how ζ is advanced in discrete time steps Δt.

$$\zeta(t + \Delta t) \approx \zeta(t) + \dot{\zeta}(t)\Delta t$$

The velocities are scaled based on the updated friction coefficient ζ. This arises from integrating the particle equations of motion, which include a friction term $-\zeta \mathbf{v}_i$.

$$\mathbf{v}_i(t + \Delta t) \approx \mathbf{v}_i(t)e^{-\zeta(t+\Delta t)\Delta t}$$

Parrinello-Rahman barostat

The goal of the Parrinello-Rahman barostat is to maintain a target pressure P_{target} by allowing the box size L (and volume $V = L^3$) to dynamically change based on the difference between the instantaneous internal pressure P_{inst} and the target pressure [9].

Instantaneous Internal Pressure (P_{inst}) is calculated from kinetic and virial contributions.

$$P_{inst}(t) = P^{kin}(t) + P^{vir}(t)$$

The change in box size is driven by the pressure difference. W is the barostat coupling constant (or "mass") controlling the volume fluctuation response speed.

$$W\ddot{L}(t) \propto V(t)(P_{inst}(t) - P_{target})$$

The box size is updated based on its equation of motion integrated over Δt.

$$L(t + \Delta t) = L(t) \times \lambda(t)$$

where $\lambda(t)$ is the scaling factor determined from the pressure difference and W.

When the box size changes, particle positions and velocities must be scaled accordingly.

$$\mathbf{r}_i(t + \Delta t) = \mathbf{r}_i(t) \times \lambda(t)$$

$$\mathbf{v}_i(t + \Delta t) = \mathbf{v}_i(t) \times \lambda(t)$$

Viscosity results with barostat

By first equilibrating the system using an NPT simulation at the target experimental pressure, we obtained an average simulation box volume. This volume, along with the final particle configuration from NPT, was used to initialize the subsequent NVT simulation, ensuring it started close to the desired thermodynamic state. Unfortunately, no improvement in plateau stability was observed.

Additionally, setting the barostat and thermostat parameters turned out to be challenging. We couldn't get good results at 107.7 K and 1296.2 kg/m3 as the temperature and pressure were not stable. Instead, we tried modeling a gas-like phase at 223 K, density 3.51 kg/m3, and pressure 0.1628 MPa. The nose-Hoover coupling constant was 4e-24 $J \cdot s^2$, and the Parrinello-Rahman coupling constant was 5e-40 $kg \cdot m^2$. We ran the NPT simulation for 2000 ps with a step length of 2 fs. We took an average volume during the simulation (fig. 12) and final configuration and set it as an initial state for the NVT simulation.

The results of the NPT-NVT simulation are in fig. 13. The autocorrelation functions fluctuate visually more compared to when only the NVT simulation was used, and again, the plateau collapsed. The results were even more off with NPT-NVT: the experimental viscosity was 17.61 μPa·s, whereas we got around 0.06 μPa·s. The more off result might not only be because we used NPT, but we were simulating very low density.

Since the barostat and thermostat parameters were difficult to tune, we did an experimental run with NVE. That way, we can be sure that the thermostats do not affect the natural dynamics. For that, we got a volume from NPT, the final frame from NVT, and simulated with a 2 fs timestep. The results are shown in fig. 14, and again, the viscosity value 0.6 μPa·s remained lower than the experimental values. In fig. 14, it can be seen that the plateau forms as the autocorrelation functions approach zero until 40 ps, but as the autocorrelations don't

fluctuate around zero but float away, the Green-Kubo viscosity is also not stable. Therefore, we got the best results by running only NVT.
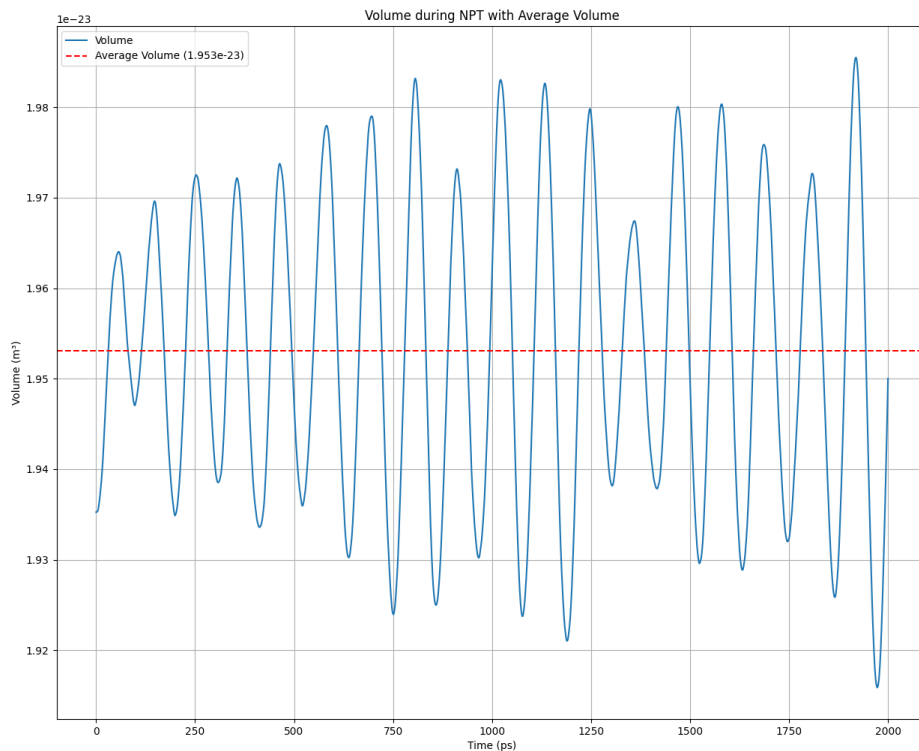

Figure 12: Volume fluctuations during NPT simulation at 223 K, 3.51 kg/m3 and 0.1628 MPa with 1024 particles. The average volume $1.953 \times 10^{-23} m^3$ was given as an input to the NVT simulation. Nose-Hoover coupling constant = 4e-24 Js^2, Parrinello-Rahman coupling constant = 5e-40 $kg \cdot m^2$.

Figure 13: The autocorrelation functions of pressure component and Green-Kubo viscosity from NPT-NVT simulation at 223 K, 3.51 kg/m^3 and 0.1628 MPa with 1024 particles.
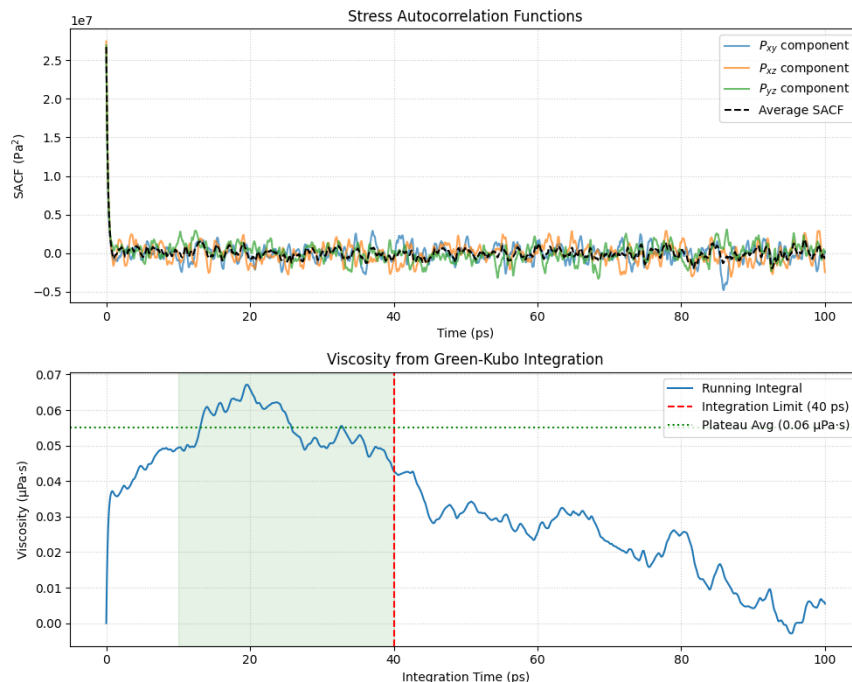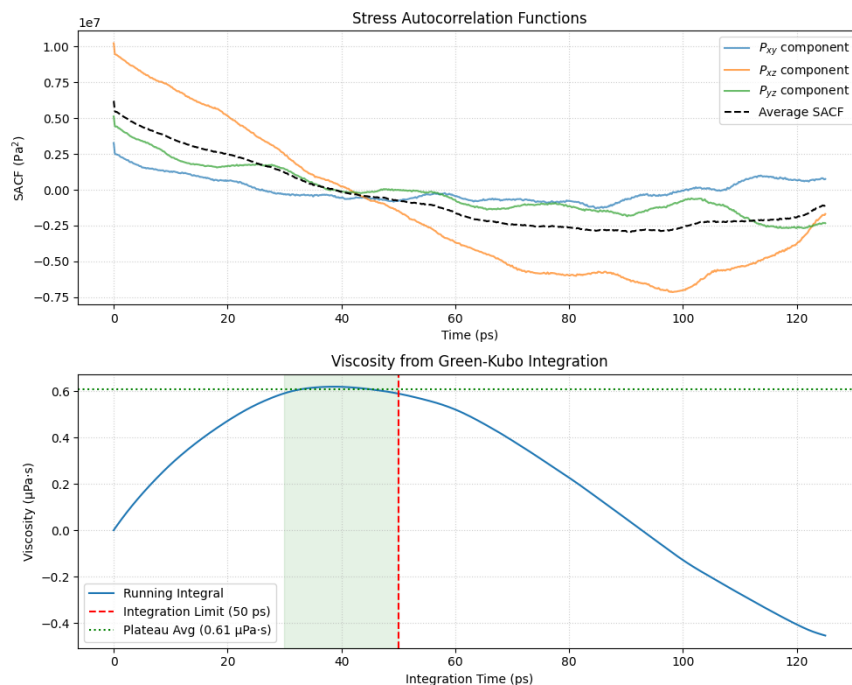

Figure 14: The autocorrelation functions of pressure component and Green-Kubo viscosity from NPT-NVT-NVE simulation at 223 K, 3.51 kg/m^3 and 0.1628 MPa with 1024 particles.

References

[1] S.-H. Lee, "Molecular dynamics simulation study of the transport properties of liquid argon: The green-kubo formula revisited," *Bulletin of the Korean Chemical Society*, vol. 28, no. 8, pp. 1371–1374, 2007.

[2] A. Michels, J. Levelt, and W. De Graaff, "Compressibility isotherms of argon at temperatures between- 25° c and- 155° c, and at densities up to 640 amagat (pressures up to 1050 atmospheres)," *Physica*, vol. 24, no. 6-10, pp. 659–671, 1958.

[3] M. Henderson and M. Wertheim, "Phase diagram and pv isotherms of argon," *The Journal of Chemical Physics*, vol. 51, no. 12, pp. 5420–5429, 1969.

[4] W. Haynes, "Viscosity of gaseous and liquid argon," *Physica*, vol. 67, no. 3, pp. 440–470, 1973.

[5] R. Kubo, "Statistical-mechanical theory of irreversible processes. i. general theory and simple applications to magnetic and conduction problems," *Journal of the physical society of Japan*, vol. 12, no. 6, pp. 570–586, 1957.

[6] R. Kubo, M. Yokota, and S. Nakajima, "Statistical-mechanical theory of irreversible processes. ii. response to thermal disturbance," *Journal of the Physical Society of Japan*, vol. 12, no. 11, pp. 1203–1211, 1957.

[7] M. S. Green, "Markoff random processes and the statistical mechanics of time-dependent phenomena. ii. irreversible processes in fluids," *The Journal of chemical physics*, vol. 22, no. 3, pp. 398–413, 1954.

[8] D. Frenkel and B. Smit, *Understanding molecular simulation: from algorithms to applications*. Elsevier, 2023.

[9] M. Parrinello and A. Rahman, "Polymorphic transitions in single crystals: A new molecular dynamics method," *Journal of Applied physics*, vol. 52, no. 12, pp. 7182–7190, 1981.